Pol. J. Environ. Stud. Vol. 29, No. 4 (2020), 2845-2853
DOI: *10.15244/pjoes/111135* ONLINE PUBLICATION DATE: 2020-02-26

Original Research

Adsorptive Removal of Textile Dye Direct Blue 9 from Aqueous Solution by Nano-Sized Polymers: Kinetic and Thermodynamic Studies

Aslı Göçenoğlu Sarıkaya*

Faculty of Science and Art, Bursa Uludag University, Görükle Campus, Bursa, Turkey

Received: 29 January 2019
Accepted: 27 July 2019

Abstract

In this study, polymeric nanoparticles were used as an adsorbent to remove the textile dye Direct Blue 9 (DB9) from an aqueous solution. Adsorption capacity of the polymeric nanoparticles were determined in various conditions such as pH, temperature, and dye concentration. Kinetic parameters were also calculated. Optimum initial pH, temperature and equilibrium time were determined as 6.0, 318 K and 90 minutes, respectively. The maximum adsorption capacity of adsorbent and percentage removal of DB9 were detected as 15.49 mg/g and 98.15%, respectively. To clarify the nature of the adsorption process isotherm, thermodynamic and kinetic studies were also performed. The adsorption process obeys the Langmuir isotherm model and pseudo-second order model.

Keywords: Direct Blue 9, adsorption; nanopolymers, removal, textile dye

Introduction

Organic dyes, which include azo dyes or complex aromatic structure [1], are widely used in the textile industry [2], pulp and paper manufacturing, printing and leather treatment [3]. However, these industrial wastes are hazardous for living organisms, especially in aquatic forms [4]. Many of them are classified as carcinogenic and toxic [5]. In general, they are biologically non-degradable, and stable to heat, light and oxidizing agents [1, 6]. Due to the inert properties of dyes, traditional treatment technologies of industrial wastewater have been improved. Coagulation/flocculation [7-9], membrane filtration [10, 11], electrochemical methods [12, 13], biodegradation [14], TiO_2 photo-catalysis [15, 16], ion exchange [17, 18] and adsorption [19, 20] processes are widely used to remove dyes from wastewater.

Because of the high removal efficiency of dye removal, adsorption is one of the most commonly used techniques to treat wastewater [21]. Adsorption gives some advantages to researchers and companies since the operation is cheap, simple and easy, with a wide field of suitable and available adsorbents allowing for adsorbent regeneration and reuse [22-25].

Durability, preservability as a long time and stability of nanopolymers have created the much-applied potential for using these structures in many areas. Activated carbon [26, 27], 'low cost adsorbents' such as agricultural solid wastes [28], biomass solid waste-based activated carbon [29], inorganic materials like clay minerals [30], siliceous materials [31], bentonites

*e-mail: agocenoglu@uludag.edu.tr

or zeolites [32, 33], biosorbents, microbial biomass [34-36] and polymeric materials [20, 37] are widely used as adsorbents. Polymeric materials, especially nano-sized polymers, are widely used as adsorbents due to their size-dependent physical and chemical properties [38].

Textile dyes are classified due to their chromophore or chemical structures such as anthraquinone, ethane, azo, and phthalocyanine. The most common one is azo dye, which is used in the textile and paper industries. Azo dyes include azo bond (R-N = N-R') and one or more aromatic rings. In general, azo dyes have mutagenic, toxic, and carcinogenic structures, thus these dyes not only affect human as carcinogens and mutagens but also affect aquatic environments. These dyes are stable and non-degradable by biological or chemical processes. Direct Blue dyes are classified into three class as mono-, di-, and tri-azo dyes [38]. Direct Blue 9 (DB9) is mainly used as dyestuff in textile industries, and the removal of these dyes is important. Various methods such as coagulation/flocculation, ion exchange, electrochemical treatment, chemical oxidation, biological treatment, and adsorption are used to remove azo dyes from wastewater [39].

This study focused on removing the toxic textile dye Direct Blue 9 (DB9) from aqueous solutions and representing the usability of poly(2-hydroxyethyl methacrylate) [poly(HEMA)] nano-sized polymers as an adsorbent. Poly(HEMA) was produced by the emulsion polymerization method and then characterized by infrared spectroscopy (IR) and scanning electron microscopy (SEM). Batch adsorption experiments were performed under various operating conditions such as pH, contact time and temperature. Adsorption isotherms and kinetic values were determined. Also, reusability of the polymer was discussed.

Experimental

Materials

Direct Blue 9 (DB9, synonym; Sirius Blue K-CFN, C.I. 24155), hydroxyethyl methacrylate (HEMA;≥99%), polyvinyl alcohol (PVA; MW: 130 000) and ethylene glycol dimethacrylate (EGDMA; 98%) were obtained from Aldrich (Steinheim, Germany). Sodium dodecyl sulfate (SDS;≥98.5%) was purchased from Sigma (Steinheim, Germany). All other chemicals were analytical grade. The chemical structure of DB9 is given in Fig. 1.

Synthesis of Poly(HEMA) Nanopolymers

Poly(HEMA) nanopolymers were synthesized by the previously given emulsion polymerization procedure [38]. First of all, in the first aqueous phase PVA, SDS and $NaHCO_3$ were dissolved in distilled water. In the second aqueous phase, PVA and SDS were dissolved in distilled water in other erlenmayer. In the oil phase,

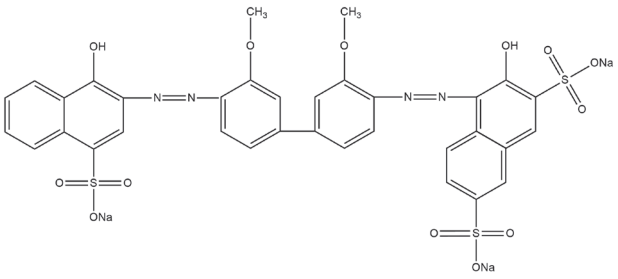

Fig. 1. Chemical structure of DB9.

HEMA was mixed with EGDMA and added to the first aqueous phase. The mixture was homogenized at 30 000 rpm (ISOLAB Homogenizer, 'Heavy Duty') for 10 minutes. The mixture was added to the second aqueous phase, and $NaHSO_3$ and $(NH_4)_2S_2O_8$ were added. The polymerization was carried out at 40ºC for 6 h. At the end of the polymerization, to remove the unreacted monomers, the polymers were washed with ethanol and water several times. Additionally, polymers were washed with distilled water and stored in water.

Characterization Studies

FT-IR analysis was performed on a Perkin Elmer Spectrum BX FTIR System. The morphology of the nanopolymers was determined by scanning electron microscope (SEM) (SEM2-Quanta 250FEG) in "Izmir Institute of Technology, Center for Materials Research".

Batch Adsorption Experiments

Initially, experiments to comment on the effect of pH on dye adsorption capacity and different pH values were carried out. The tested initial pH values (3.0 to 8.0) were prepared with acetate (0.1 M $NaCH_3COO/CH_3COOH$) or phosphate (0.1 M NaH_2PO_4/Na_2HPO_4) buffers. The dye concentration of these solutions was 30 mg/L. Suspensions were stirred at 25ºC for 3 h in a heated incubator (125 rpm).

To determine the optimum dye concentration, the suspensions were prepared by adding poly(HEMA) (1 mg) to 1 mL DB9 solutions (1.0 to 50.0 mg/L) at optimum pH. The suspensions were placed in a heated incubator at 25ºC under stirring at 125 rpm. The amount of dye adsorbed (q_e) and percentage removal (% R) of DB9 were calculated using Eqs. (1) and (2), respectively:

$$q_e = \frac{(C_0 - C_e)V}{m} \quad (1)$$

$$\%\ Removal\ = \frac{(C_0 - C_e)}{C_0} \times 100 \quad (2)$$

…where q_e is the amount of dye in mg per gram of adsorbent, and C_0 and C_e are initial and final

concentrations of dye (mg/L), respectively. V is the volume of the dye solution (mL) and m is the mass of the adsorbent (g).

Adsorption Isotherms

The Langmuir sorption isotherm is applied to equilibrium sorption assuming monolayer sorption onto a surface with a limited number of identical binding sites. The Langmuir equation (Eq. 3) is written as [38]:

$$\frac{C_e}{q_e} = \frac{1}{Q_L K_L} + \frac{C_e}{Q_L} \quad (3)$$

…where K_L is Langmuir constant (L/mg), Q_L is the maximum adsorption at monolayer coverage (mg/g), q_e is dye concentration at equilibrium onto adsorbent (mg/g) and C_e is dye concentration at equilibrium in solution (mg/L).

The Freundlich sorption isotherm equation for heterogeneous surface energy systems is given by Eq. 4 [38]:

$$\ln q_e = \ln K_F + \frac{1}{n} \ln C_e \quad (4)$$

…where q_e is dye concentration at equilibrium onto adsorbent (mg/g) and C_e is dye concentration at equilibrium in solution (mg/L). K_F and n are Freundlich constants, determined from the plot of ln q_e versus ln C_e. The parameters K_F and $1/n$ correlate with sorption capacity and the sorption intensity of the system. The magnitude of the term ($1/n$) gives evidence to the availability of the sorbent/adsorbate systems [40].

The Sips sorption isotherm equation was given in Eq. 5. This equation was derived from the limiting behavior of Langmuir and Freundlich isotherms [41].

$$\frac{1}{q_e} = \frac{1}{Q_{max}\, K_S} \left(\frac{1}{C_e}\right)^{1/n} + \frac{1}{Q_{max}} \quad (5)$$

…where q_e is dye concentration at equilibrium onto adsorbent (mg/g) and C_e is dye concentration at equilibrium in solution (mg/L). K_s is Sips constant (L/mg) and Q_{max} is maximum adsorption capacity (mg/g).

Recyclability of the Adsorbent

The recyclability of the adsorbent was performed by repeated adsorption/desorption cycles using the same adsorbent in the same dye solution at five times. As a desorption agent sodium acetate buffer was used. A constant dosage of polymer (1 mg) was placed in 5 mL dye solution (50 mg/L) and kept in contact for 3 h. For each cycle, the adsorption capacity was calculated.

Results and Discussion

Characterization of the Poly(HEMA)

The FTIR spectra of before and after adsorption from a range of 600-4000 cm^{-1} is given in Fig. 2. The bands observed at about 3320 cm^{-1} could be assigned O-H stretching vibration. The bands at 2949 cm^{-1} shifts to 2955 cm^{-1} representing C-H stretching of CH_3. The strong band of C=O and C-O stretching vibration peaks are observed at 1716 and 1240 cm^{-1}, respectively.

To determine the surface texture and morphology of the adsorbent, scanning electron microscopy (SEM) images were taken before and after adsorption of DB9. The results obviously show that the polymers are spherical and in nano-size with smooth surface. As seen in Fig. 3, the adsorbent has homogeneity, which is supposed to be the active site for DB9 binding. SEM images also revealed that the surface of polymeric adsorbent is flattened after DB9 adsorption.

Effect of pH on Dye Adsorption

The textile dyes have different aromatic rings and functional groups (such as nitro, azo or metal) [1, 42]. The pH of a dye solution is an important effecting factor for adsorption [36, 43]. The ionization of the adsorptive molecule and adsorbent can effectively

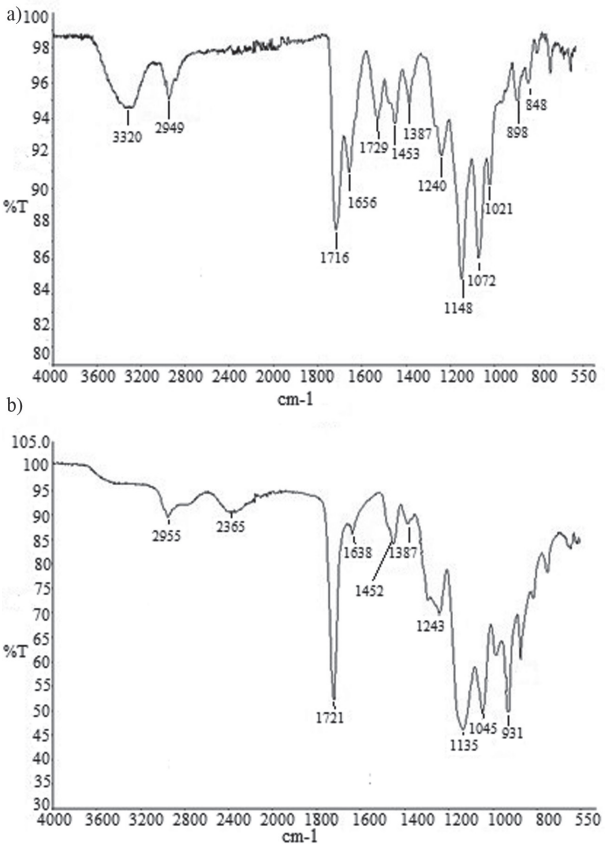

Fig. 2. FT-IR spectrum of poly(HEMA) a) before and b) after adsorption of DB9.

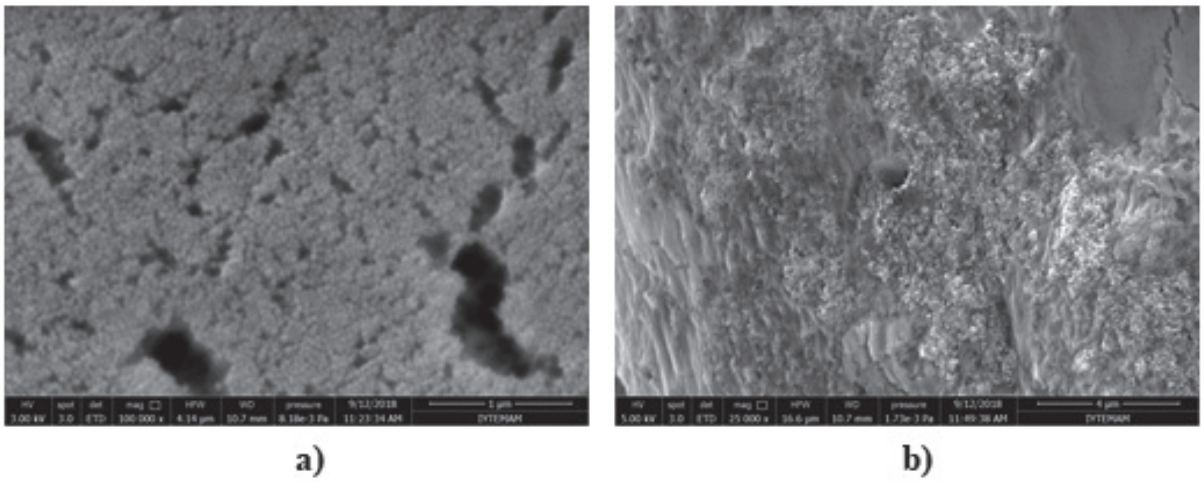

Fig. 3. SEM images of poly(HEMA) a) before and b) after adsorption of DB9.

change by the variation of the pH solution, hence the dye adsorption is dependent on the solution pH [44, 45]. Fig. 4 shows the effect of pH on adsorption of dye onto the polymer. The maximum adsorption and removal of dye were observed at pH 6.0. The adsorption capacities of poly(HEMA) increased with pH until the pH reached 6.0, and then the adsorption capacities decreased with increasing pH. The maximum adsorption capacity was determined at pH 6.0. However, the ionizable groups of dye and poly(HEMA) (hydroxyl groups) are responsible from the electrostatic interactions and hydrogen bonds between dye and polymer.

Effect of Initial Dye concentration and Contact Time on Dye Adsorption

To determine the optimum dye concentration, the DB9 solutions ranging from 1.0 to 50.0 mg/L were studied with an amount of 1 mg poly(HEMA) and 1 mL dye solution at optimum pH at 298 K. With an increase in the initial DB9 concentration from 1.0 to 50.0 mg/L, the adsorption capacity (q_e) and percentage removal (*%R*) at equilibrium increased from 4.07 mg/g to 22.54 mg/g, and 37.37% to 98.86% at 298 K, respectively. The results were given in Fig. 5.

The effect of contact time on the adsorption capacities of dye onto poly(HEMA) and removal percentage at 277, 298 and 318 K are shown in Fig. 6a) and Fig. 6b), respectively. The adsorbed amounts of dyes increased with an increase in both contact time and temperature. Adsorption process was completed within 90 min and no remarkable changes were observed until 180 min. Lots of free adsorbent sites are available for adsorption and thus dye molecules can affectively adsorb onto these sites, rapidly increasing the temperature. 82.30%, 94.07% and 98.15% DB9 removal takes place at 277, 298 and 318 K in 1 80 min, respectively. The adsorption capacities of the poly(HEMA) are 12.98, 14.84 and 15.49 mg/g at 277, 298 and 318 K, respectively.

Effect of Adsorbent Dosage and Agitation Rate

To determine the effect of adsorbent dosage for adsorption capacity and percentage removal of DB9 from an aqueous solution, the different adsorbent values ranging from 0.5 mg to 8 mg were used in the adsorption process. The initial concentration of DB9 was 25 mg/L and the contact time was 180 minutes at

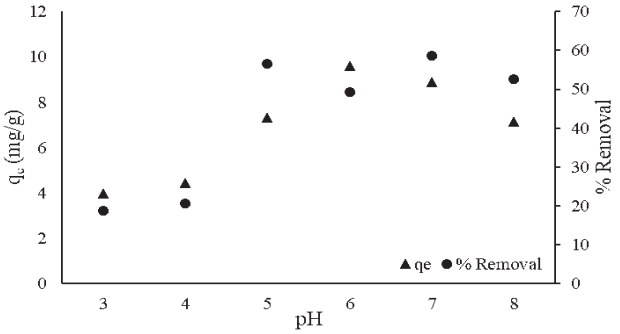

Fig. 4. Effect of pH for adsorption capacity (q_e) and percentage removal (*% R*) of DB9 onto poly(HEMA).

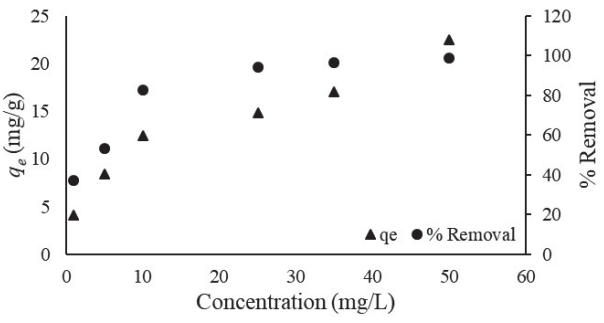

Fig. 5. Effect of initial DB9 concentration for adsorption capacity (q_e) and percentage removal (*% R*) of DB9 onto poly(HEMA).

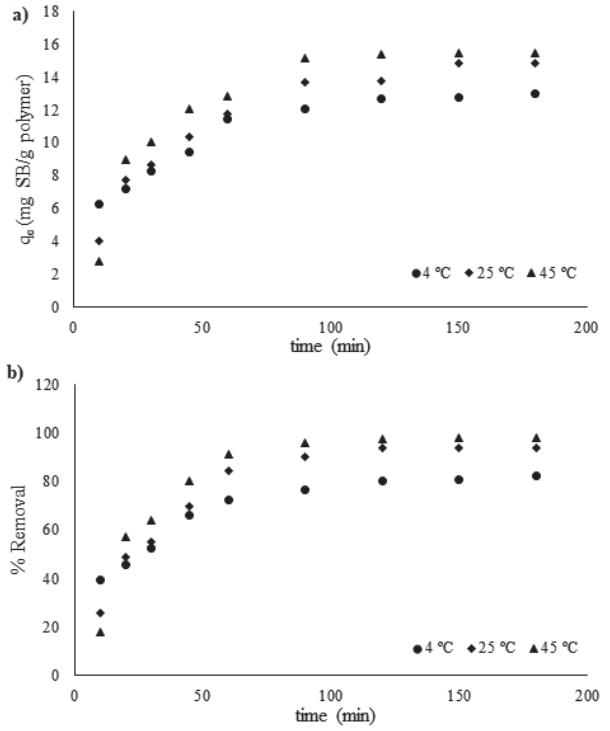

Fig. 6. Effect of contact time and temperature onto a) adsorption capacity (q_e) and b) percentage removal (*% R*) for adsorption of DB9 onto poly(HEMA).

298 K. The results were given in Fig. 7. With increasing the amount of adsorbent from 0.5 mg to 8 mg, q_e and percentage *R* increased from 3.85 mg/g to 28.63 mg/g, and from 86.43% to 99.70%, respectively. Increase in the percentage *R* and q_e with adsorbent dosage can be based on increased adsorbent surface area and adsorption sites.

To determine the effect of agitation speed for adsorption of DB9 in the range of 75-150 rpm, agitation rates were investigated during the adsorption process. The adsorbent dosage was 1 mg, the total initial DB9 concentration 25 mg/L, and the contact time was 180 minutes at 298 K. The results are given

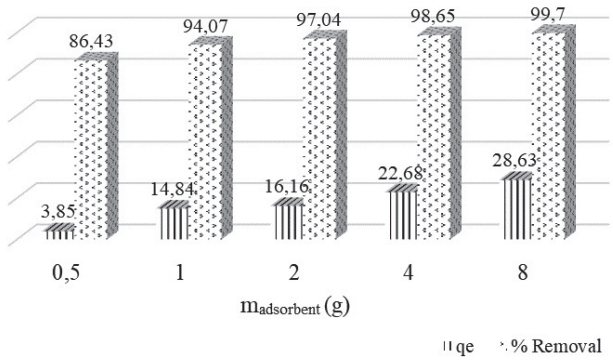

Fig. 7. Effect of adsorbent dosage for adsorption capacity (q_e) and percentage removal (*% R*) of DB9 onto poly(HEMA).

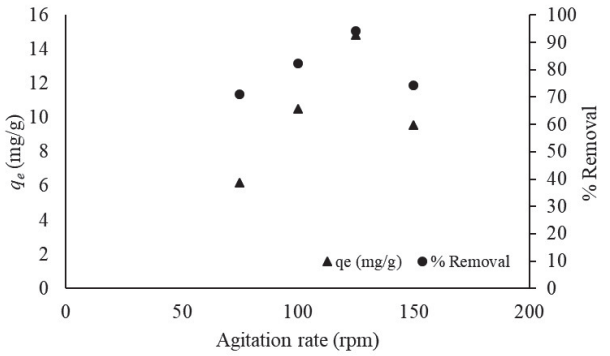

Fig. 8. Effect of agitation rate for adsorption capacity (q_e) and percentage removal (*% R*) of DB9 onto poly(HEMA).

in Fig. 8. The maximum removal of DB9 occurred at 125 rpm. Agitation of solution helps for better interaction between binding sites of both adsorbent and dye molecules, so these molecules penetrate to deeper layers of the adsorbent. When the agitation rate exceeded the optimum speed, the interaction between adsorbent and dye molecules decreased [46].

Adsorption Isotherms

The adsorption capacity and other parameters were evaluated using Langmuir, Freundlich and Sips isotherm models. The adsorption capacity (q_e) was determined as 16.24 mg/g (Table 1). The high value of correlation coefficient (0.987) point at the practicality of Langmuir isotherm which supposes uniform activity distribution and a monolayer coverage on the sorbent surface. R_L values also support the adsorption of dye onto poly(HEMA) (Table 1).

The equilibrium data were also fitted to the Freundlich isotherm model. The parameters K_F and *n* are 0.226 and 1.392, respectively. 1/*n* gives an indication of the suitability of the sorbent/adsorbate systems [47].

Adsorption Thermodynamics

Thermodynamic parameters such as free energy change (ΔG), enthalpy changes (ΔH) and entropy changes (ΔS) were calculated using the Van't Hoff equation at various temperatures [48] (Eq. 6):

$$\ln K_L = -\frac{\Delta H^0}{RT} + \frac{\Delta S^0}{R} \tag{6}$$

…where K_L is the Langmuir equilibrium constant, *T* is the absolute temperature (K) and *R* is the universal gas constant (8.314 J/mol K). ΔH^0 and ΔS^0 can be determined from the slope and intercept of the plot of ln K_L versus 1/*T*. The ΔG^0 of the adsorption was calculated using Eq. 7:

$$\Delta G^0 = \Delta H^0 - T\Delta S^0 \tag{7}$$

Table 1. Adsorption isotherm models for DB9 adsorption onto poly(HEMA).

	Langmuir Isotherm Model			Freundlich Isotherm Model			Sips Isotherm Model		
Temperature (K)	K_L x 10^2 (L/mg)	Q_L (mg/g)	R^2	K_F (L/mg)	n	R^2	K_S x 10^2 (L/mg)	Q_{max} (mg/g)	R^2
298	4.68	16.24	0.987	0.226	1.392	0.928	11.54	0.575	0.954

Table 2. Thermodynamic parameters for DB9 adsorption onto poly(HEMA).

T (K)	ΔG^o (kJ/mol)	ΔH^o (kJ/mol)	ΔS^o (J/mol.K)
277	-1.716	2.276	14.412
298	-2.018		
318	-2.307		

The data are listed in Table 2. The positive ΔH^0 depicted that the dye adsorption on polymeric adsorbent was endothermic. The negative ΔG^0 indicates that the adsorption process occurs spontaneously. Besides the positive value of entropy change, (ΔS^0) defines the affinity of adsorbent for the dye.

Adsorption Kinetics

Adsorption kinetics is one of the important parameters for investigating the mechanism of adsorption [49]. In this study, pseudo first-order, pseudo second-order, and intraparticle diffusion kinetic models were used to clarify the adsorption kinetics.

The pseudo first- and second-order kinetic models are expressed at Eq. 8 and Eq. 9, respectively:

$$\ln(q_e - q_t) = \ln q_e - k_1 t \quad (8)$$

$$\frac{t}{q_t} = \frac{1}{k_2 q_e^2} + \frac{t}{q_e} \quad (9)$$

…where q_e is the amount of dye adsorbed by polymer at equilibrium condition (mg/g), q_t is the amount of dye adsorbed by polymer at time t (min), and k_1 (1/min) and k_2 (g/mg min) are the equilibrium rate constants for pseudo first- and second-order kinetic models, respectively. For the pseudo first-order kinetic model, k_1 and q_e are obtained from the slope and intercept of the plot of $ln(q_e\text{-}q_t)$ versus t, respectively [50]. For the pseudo second-order kinetic model, k_2 and q_e are determined from the slope and intercept of the plot of t/q_t versus t, respectively [51, 52].

The intraparticle diffusion model explains that the adsorption process occurs in several steps involving the transport of solute molecules from bulk aqueous phase to the surface of the adsorbent particles, which is followed by diffusion of the molecules into the interior of the solid pores [43, 51]. For most adsorption processes, the amount of adsorption is commensurate to $t^{1/2}$ rather than with the contact time. This model can be expressed at Eq. 10:

$$q_t = k_{id} t^{1/2} \quad (10)$$

…where q_t is the adsorption capacity at time t (min), $t^{1/2}$ is the half-life time in second and k_{id} is the intraparticle diffusion rate constant (mg/g $min^{1/2}$) at different initial dye concentrations. k_{id} can be calculated from the slope of the plot. The adsorption kinetic models and parameters are given in Table 3.

According to the results, the best-fit kinetic model can be chosen dependent upon the linear regression correlation coefficient (R^2) values. Furthermore, q_e values are closed to experimental q_e values in the pseudo second-order kinetic model. Usually for most adsorption systems, the pseudo second-order kinetic model is better and well represented [51]. For removing textile dyes from aqueous solutions a great number of adsorbents such as ash, polymeric particles or microbial biomass can be used effectively. Adsorption capacities of various adsorbents for different kinds of dyes are given in Table 4.

Recyclability of the Adsorbent

One of the important parameters in adsorption-based processes is desorption and reusability of the adsorbent.

Table 3. Adsorption kinetic models and parameters for removal of DB9 onto poly(HEMA).

Parameters Temperature (K)	Experimental q_e (mg/g)	Pseudo-first order kinetic model			Pseudo-second order kinetic model			Intraparticle diffusion model	
		k_1 x 10^2 (1/min)	q_e (mg/g)	R^2	k_2 x 10^2 ((g/mg)/min)	q_e (mg/g)	R^2	k_{id}	R^2
277	12.983	2.62	2.188	0.9865	7.01	11.87	0.9981	0.68	0.8908
298	14.841	4.67	3.0436	0.9671	5.68	15.24	0.9922	1.02	0.8522
318	15.486	3.65	3.0243	0.9547	5.19	18.59	0.9663	1.09	0.8315

Table 4. Adsorption capacities of various adsorbents for different kinds of dyes.

Adsobent	Dye	q_e	*% R*	Reference
KT3B kaolin	MB	52.76 mg/g	-	52
Trimellitated-sugarcane bagasse	Auramine-O Safranin-T	1.005 mmol/g 0.638 mmol/g	- -	53
Chitosan-based composite hydrogel	Rhodamine 6G	-	87.31	54
Coal fly ash	Indigo carmine	1.48 mg/g	-	55
Calcium hydroxide	Indigo carmine	0.95 mg/g	-	56
Activated carbon-entrapped microfibrilated cellulose film	brilliant red 5GN	19.30 mg/g	-	57
Ni/C nanoparticles	Rhodamine B Methylene Blue	3.935 mg/g 5.204 mg/g	-	58
poly (N-isopropylacrylamide)-co-acrylic acid microgel	Orange II	-	% 29.5	59
poly HEMA–chitosan-MWCNT nano-composite	Methyle orange	306 mg/g	-	60
Lyophilized *Trametes versicolor* biomass	Sirius Blue K-FCN	62.62 mg/g	-	42
Poly(HEMA) nanoparticles	Direct Blue 9	15.49 mg/g	98.15 %	This study

It is required that the desorption agent does not damage the adsorbent or affect adsorption capacity. In this study, the recyclability experiment of DB9 was carried out. Sodium acetate buffer was used as a desorption agent in the recyclability studies. The DB9 adsorbed polymers were shaken at room temperature for 3 h. It was found that during a 5 adsorption-desorption cycle the adsorption capacity of the nanopolymer decreased only 5.5%.

Conclusions

In this study, poly(HEMA) nanopolymers were produced, characterized and investigated regarding their abilities to remove textile dye Direct Blue 9 (DB9) in aqueous solution for the first time. The optimum pH and temperature for adsorption of DB9 from aqueous solution were determined as 6.0 and 318 K, respectively. All experiments were achieved at pH 6.0. Increasing the temperature from 277 K to 318 K, the maximum adsorption capacity was also increased from 12.98 mg/g to 15.49 mg/g and percentage removal of DB9 from 82.30% to 98.15%, respectively. Results obtained indicate that the adsorption process is fast and spontaneous within the first 90 min. Isotherm, thermodynamic and kinetic studies were performed to clarify the nature of the adsorption process. The experimental data supports the pseudo second-order model. The adsorption process is fitted to the Langmuir isotherm model. In addition, the mean values of thermodynamic parameters of standard free energy, standard enthalpy (ΔH^0= 2.276 kJ mol^{-1}) and standard entropy (ΔS^0= 14.412 J mol^{-1}K^{-1}) of the adsorption mechanism were determined. In conclusion, poly(HEMA) was examined as an adsorbent for the adsorption of a textile dye, Direct Blue 9, in aqueous solutions at the first time and reported the suitability of the poly(HEMA) as an adsorbent.

Acknowledgements

This study was performed at the Department of Biochemistry Faculty of Science Ege University, Izmir, Turkey. Special thanks to Prof. Dr. Nurdan Kaşıkara Pazarlıoğlu, Assistant Prof. Alper Akkaya and Dr. Emre Erden.

Conflict of Interest

The authors declare no conflict of interest.

References

1. KADAM A.A., LEE D.S. Glutaraldehyde cross-linked magnetic chitosan nanocomposites: Reduction precipitation synthesis, characterization, and application for removal of hazardous textile dyes. Biosour. Technol. **193**, 563, **2015**.
2. ELMOUBARKI R., MAHJOUBI F.Z., TOUNSADI H., MOUSTADRAF J., ABDENNOURI M., ZOUHRI A., EL ALBANI A., BARKA N. Adsorption of textile dyes on raw and decanted Moroccan clays: Kinetics, equilibrium and thermodynamics. Water Resources and Industry. **9**, 16, **2015**.
3. BANERJEE S., CHATTOPADHYAYA M.C. Adsorption characteristics for the removal of a toxic dye, tartrazine from aqueous solutions by a low-cost agricultural by-product. Arab. J. Chem. **10**, S1629, **2017**.
4. SHAJAHAN A., SHANKAR S., SATHIYASEELAN A., NARAYAN K.S., NARAYANAN V., KAVIYARASAN

V., IGNACIMUTHU S. Comparative studies of chitosan and its nanoparticles for the adsorption efficiency of various dyes. Int. J. Biol. Macromol. **104**, 1449, **2017**.
5. HUANG R., LIU Q., HUO J., YANG B. Adsorption of methyl orange onto protonated crosslinked chitosan. Arab. J. Chem. **10**, 24, **2017.**
6. SUBRAMANI S.E., THINAKARAN N. Isotherm, Kinetic and thermodynamic studies on the adsorption behaviour of textile dyes onto chitosan. Process Saf. Environ. **106**, 1, **2017**.
7. YANG R., LI H., HUANG M., YANG H., LI A. A review on chitosan-based flocculants and their applications in water treatment. Water Res. **95**, 59, **2016**.
8. DAO V.H., CAMERON N.R., SAITO K. Synthesis, properties and performance of organic polymers employed in flocculation applications. Polym. Chem. **7** (1), 11, **2016**.
9. DOTTO J., VEIT M.T., MORENO PALACIO S., BERGAMASCO R. Performance of different coagulants in the coagulation/flocculation process of textile wastewater. J. Clean. Prod. **208**, 656, **2019**.
10. FANE A.G., WANG R., HU M.X. Synthetic membranes for water purification: status and future. Angew. Chem. Int. Ed. **54** (11), 3368, **2015**.
11. PEYDAYESH M. MOHAMMADI T., BAKHTIARI O. Effective treatment of dye wastewater via positively charged TETA-MWCNT/PES hybrid nanofiltration membranes. Sep. Purif. Technol. **194**, 488, **2018**.
12. EL-ASHTOUKHY E.-S. Z., AMIN N. K., ABD EL-LATIF M.M., BASSYOUNI D.G. HAMAD H.A. New insights into the anodic oxidation and electrocoagulation using a self-gas stirred reactor: a comparative study for synthetic C.I Reactive Violet 2 wastewater. J. Clean. Prod. **167**, 432, **2017**.
13. BASSYOUNI D.G., HAMAD H.A., EL-ASHTOUKHY E.-S.Z., AMIN N.K., ABD EL-LATIF M.M. Comparative performance of anodic oxidation and electrocoagulation as clean processes for electrocatalytic degradation of diazo dye Acid Brown 14 in aqueous medium. J. Hazard. Mater. **335**, 178, **2017**.
14. SPASIANO D., SICILIANO A., RACE M., MAROTTA R., GUIDA M., ANDREOZZI R., PIROZZI F. Biodegradation, ecotoxicity and UV_{254}/H_2O_2treatment of imidazole, 1-methyl-imidazole and N,N′-alkyl-imidazolium chlorides in water. Water Res., **106**, 450, **2016**.
15. HAMAD H.A., ABD EL-LATIF M.M., KASHYOUT A.B., SADIK W.A., FETEHA M.Y. Optimizing the preparation parameters of mesoporous nanocrystalline titania and its photocatalytic activity in water: physical properties and growth mechanisms. Process Saf. Environ. Prot. **98**, 390, **2015**.
16. HAMAD H.A., SADIK W.A., ABD EL-LATIF M.M., KASHYOUT A.B., FETEHA M.Y. Photocatalytic parameters and kinetic study for degradation of dichlorophenol-indophenol (DCPIP) dye using highly active mesoporous TiO_2 nanoparticles. J. Environ. Sci. **43**, 26, **2016**.
17. ELKADY M., SHOKRY H., HAMAD H. Effect of superparamagnetic nanoparticles on the physicochemical properties of nano hydroxyapatite for groundwater treatment: adsorption mechanism of Fe(II) and Mn(II). RSC Adv. **6**, 82244, **2016**.
18. ZHAO S.-N., KRISHNARAJ C., JENA H. J., POELMAN D., VAN DER VOORT P. An anionic metal-organic framework as a platform for charge-and size-dependent selective removal of cationic dyes. Dyes Pigments. **156**, 332, **2018**.
19. EL ESSAWY N.A., ALI S.M., FARAG H.A., KONSOWA A.K., ELNOUBY M., HAMAD H.A. Green synthesis of graphene from recycled PET bottle wastes for use in the adsorption of dyes in aqueous solution. Ecotox. Environ. Saf. **145**, 57, **2017**.
20. MURRAY A., OMERCI B. Competitive effects of humic acid and wastewater on adsorption of Methylene Blue dye by activated carbon and non-imprinted polymers. J. Environ Sci. **66**, 310, **2018**.
21. HAMAD H., BASSYOUNI D., EL-ASHTOUKHY E.-S., AMIN N., ABD EL-LATIF M. Electrocatalytic degradation and minimization of specific energy consumption of synthetic azo dye from wastewater by anodic oxidation process with an emphasis on enhancing economic efficiency and reaction mechanism. Ecotox. Environ. Safe. 148, 501, **2018**.
22. MONTE BLANCO S.P.D., SCHEUFELE F.B., MÓDENES A.N., ESPINOZA-QUIÑONES F.R., MARIN P., KROUMOV A.D., BORBA C.E. Kinetic, equilibrium and thermodynamic phenomenological modeling of reactive dye adsorption onto polymeric adsorbent. Chem. Eng. J. **307**, 466, **2017**.
23. PATHANIA D., SHARMA S., SINGH P. Removal of methylene blue by adsorption onto activated carbon developed from *Ficus carica* bast., Arab. J. Chem. **10**, 1445, **2017**.
24. TANG Y., YANG R., MA D., ZHOU B., ZHU L., YANG J. Removal of methyl orange from aqueous solution by adsorption onto a hydrogel composite. Polym. Polym. Compos. **26** (2), 161, **2018**.
25. TORGUT G., DEMIRELLI K. Comparative adsorption of different dyes from aqueous solutions onto polymer prepared by rop: kinetic, equilibrium and thermodynamic studies. Arab. J. Sci. Eng. **43**, 3503, **2018**.
26. PAVAS E.G., DOBROSZ-GOMEZ I., GOMEZ-GARCIA M.-A., Optimization and toxicity assessment of a combined electrocoagulation, H_2O_2/Fe^{2+}/UV and activated carbon adsorption for textile wastewater treatment. Sci. Total Environ. **651** (1), 551, **2019**.
27. DERYLO-MARCZEWSKA A., BLACHNIO M., MARCZEWSKI A. W., SECZKOWSKA M., TARASIUK B. Phenoxyacid pesticide adsorption on activated carbon – Equilibrium and kinetics. Chemosphere. **214**, 349, **2019**.
28. AFROZE S., SEN T.K. A Review on Heavy Metal Ions and Dye Adsorption from Water by Agricultural Solid Waste Adsorbents. Water Air Soil Pollut. **229** (7), 225, **2018**.
29. BAYSAL M., BILGE K., YILMAZ B., PAPILA M., YURUM Y. Preparation of high surface area activated carbon from waste-biomass of sunflower piths: Kinetics and equilibrium studies on the dye removal, J. Environ Chem. Eng. **6** (2), 1702, **2018**.
30. CHAARI I., FAKHFAKH E., MEDHIOUB M., JAMOUSSI F. Comparative study on adsorption of cationic and anionic dyes by smectite rich natural clays. J. Mol. Struct. **1179**, 672, **2019**.
31. LIU S., CHEN X., AI W., WEI C. A new method to prepare mesoporous silica from coal gasification fine slag and its application in methylene blue adsorption. J. Clean. Prod. **212**, 1062, **2019**.
32. SHABAN M., ABUKHADRA M.R., SHAHIEN M.G., IBRAHIM S.S. Novel bentonite/zeolite-NaP composite efficiently removes methylene blue and Congo red dye. Environ. Chem. Lett. **16**, 275, **2018**.
33. MAHMOODI M.N., SAFFAR-DASTGERDI M.H. Zeolite nanoparticle as a superior adsorbent with high capacity:

Synthesis, surface modification and pollutant adsorption ability from wastewater. Microchem. J. **145**, 74, **2019**.
34. JAIN S.N., GOGATE P.R. Efficient removal of Acid Green 25 dye from wastewater using activated *Prunus Dulcis* as biosorbent: Batch and column studies, J. Environ. Manage. **210**, 226, **2018**.
35. ROY U., MANNA S., SENGUPTA S., DAS P., DATTA S., MUKHOPADHYAY A., BHOWAL A. Dye Removal Using Microbial Biosorbents, Green Adsorbents for Pollutant Removal. **2018**.
36. RANGABHASHIYAM S., SUJATA L., BALASUBRAMANIAN P. Biosorption characteristics of methylene blue and malachite green from simulated wastewater onto *Carica papaya* wood biosorbent. Surf. Interface. **10**, 197, **2018**.
37. SAMADI N., HASANZADEH R., RASAD M. Adsorption isotherms, kinetic, and desorption studies on removal of toxic metal ions from aqueous solutions by polymeric adsorbent. J. Appl. Polym. Sci. 41642 **2015**.
38. GÖÇENOĞLU SARIKAYA A. Removal of diazo-dye Direct Blue 2 (DB2) in aqueous solution by P(HEMA) nanoparticles. J. BAUN Inst. Sci. Technol. **21** (1), 278, **2019**.
39. MOGHADDAM S.S., MOGHADDAM M.R., ARAMI M. Coagulation/flocculation process for dye removal using sludge from water treatment plant: Optimization through response surface methodology. J. Hazard. Mater. **175** (1-3), 651, **2010**.
40. LANGMUIR I. The adsorption of gases on plane surfaces of glass, mica and platinum. JACS. **40,** 1361, **1918**.
41. FREUNDLICH H. Over the adsorption in solution. J. Phys. Chem. **57**, 385, **1906**.
42. ERDEN E., KAYMAZ Y., KASIKARA PAZARLIOGLU N. Biosorption kinetics of a direct azo dye Sirius Blue K-CFN by *Trametes versicolor*. Electron. J. Biotechn. **14** (2), 1, **2011**.
43. BENSALAH H., BEKHEET M.F., YOUNSSI S.A., OUAMMOU M., GURLO A., Removal of cationic and anionic textile dyes with Moroccan natural phosphate. J. Environ. Chem. Eng. **5**, 2189, **2017**.
44. MAHMOUD M.E., NABIL G.M., EL-MALLAH N.M., BASSIOUNY H.I., KUMAR S., ABDEL-FATTAH T.M., Kinetics, isotherm, and thermodynamic studies of the adsorption of reactive red 195 a dye from water by modified switchgrass biochar adsorbent. J. Ind. Eng. Chem. **37,** 156, **2016**.
45. SALLEH M.A.M. MAHMOUD D.K., KARIM W.A.W.A., IDRIS A. Cationic and anionic dye adsorption by agricultural solid wastes: A comprehensive review. Desalination. **280** (1), 1, **2011**.
46. ACHAK M., HAFIDIB A., OUAZZANIA N., SAYADIC S., MANDIA L. Low cost biosorbent "banana peel" for the removal of phenolic compounds from olive mill wastewater: Kinetic and equilibrium studies. J. Hazar. Mater. **166**, 117, **2009**.
47. TAHIR M.A., BHATTI H.N., IQBAL M. Solar Red and Brittle Blue direct dyes adsorption onto Eucalyptus angophoroides bark: Equilibrium, kinetics and thermodynamic studies. J. Environ. Chem. Eng. **4**, 2431, **2016**.
48. AL-DEGS Y.S., EL-BARGHOUTHI M.I., ISSA A.A., KHRAISHEH M.A., WALKER G.M. Sorption of Zn(II), Pb(II), and Co(II) using natural sorbents: Equilibrium and kinetic studies. Water Res. **40** (14), 2645, **2006**.
49. CHEN L., BAI B. Equilibrium, kinetic, thermodynamic, and in situ regeneration studies about Methylene Blue adsorption by the raspberry-like TiO_2-yeast microspheres. Ind. Eng. Chem. Res. **52**, 15568, **2013**.
50. SHENVI S.S., ISLOOR A.M., ISMAIL A.F., SHILTON S.J., AL AHMED A. Humic acid based biopolymeric membrane for effective removal of Methylene Blue and Rhodamine B. Ind. Eng. Chem. Res. **54** (18), 4965, **2015**.
51. YAGUB M.T., SEN T.K., AFROZE S., ANG H.M. Dye and its removal from aqueous solution by adsorption: A review. Adv. Colloid Interfac. **209**, 172, **2014**.
52. MOUNI L., BELKHIRI L., BOLLINGER J.C., BOUZAZA A., ASSADI A., TIRRI A., DAHMOUNE F., MADANI K., REMINI H. Removal of Methylene Blue from aqueous solutions by adsorption on kaolin: Kinetic and equilibrium studies. Appl. Clay Sci. **153** (1), 38, 2018.
53. APARECIDA FIDELES R., DIAS FERREIRA G.M., TEODORO F.S., HERRERA ADARME O.F., MENDESDA SILVA L.H., GIL L.F., ALVES GURGEL L.V. Trimellitated sugarcane bagasse: A versatile adsorbent for removal of cationic dyes from aqueous solution. Part I: Batch adsorption in a monocomponent system J. Colloid. Interf. Sci. **515**, 172, **2018**.
54. BHULLAR N., KUMARI K., SUD D. A biopolymer-based composite hydrogel for rhodamine 6G dye removal: its synthesis, adsorption isotherms and kinetics. Iran. Polym. J. **27** (7), 527, **2018**.
55. de CARVALHO T.E., FUNGARO D.A., MAGDALENA C.P., CUNICO P. Adsorption of indigo carmine from aqueous solution using coal fly ash and zeolite from fly ash. J. Radioanal. Nucl. Chem. **289**, 617, **2011**.
56. RAMESH T.N., KIRANA D.V., ASHWINI A., MANASA T. Calcium hydroxide as low cost adsorbent for the effective removal of indigo carmine dye in water. J. Saudi. Chem. Soc. **21**, 165, **2015**.
57. PEI Y., WU X., XU G., CHEN M., ZHANG Z., ZHENG X., LIU J., TANG K. Activated carbon-entrapped microfibrilated cellulose films as an effective adsorbent for removing organic dye from aqueous effluent, J. Wood Chem. Technol. **38** (1), 15, **2018**.
58. KIM T.S., SONG H.J., DAR M.A., LEE H.J., KIM D.W. Fast adsorption kinetics of highly dispersed ultrafine nickel/carbon nanoparticles for organic dye removal. Appl. Surf. Sci. **439**, 364, **2018**.
59. PARASURAMAN D., SERPE DEEPIKA M.J. Poly (N-Isopropylacrylamide) microgels for organic dye removal from water. ACS Appl. Mater. Interfaces. **3**, 2732, **2011**.
60. MAHMOODIAN H., MORADI O., SHARIATZADEHA B., SALEHF T.A., TYAGI I., MAITY A., VINOD V. A., GUPTA K. Enhanced removal of methyl orange from aqueous solutions by poly HEMA-chitosan-MWCNT nano-composite J. Mol. Liq. **202**, 189, **2015**.